IOP Publishing Semiconductor Science and Technology
Semicond. Sci. Technol. 32 (2017) 085011 (7pp) https://doi.org/10.1088/1361-6641/aa7a4c

Landau-level mixing, floating-up extended states, and scaling behavior in a GaAs-based two-dimensional electron system containing self-assembled InAs dots

Chieh-Wen Liu[1], Chieh-I Liu[1], C-T Liang[1,6], Gil-Ho Kim[2,6], C F Huang[3], D R Hang[4], Y H Chang[1] and D A Ritchie[5]

[1] Graduate Institute of Applied Physics, National Taiwan University, Taipei 106, Taiwan
[2] School of Electronic and Electrical Engineering and Sungkyunkwan Advanced Institute of Nanotechnology (SAINT), Sungkyunkwan University, Suwon, 16419, Republic of Korea
[3] 2nd Patent Division, Intellectual Property Office, Ministry of Economic Affairs, Taipei 106, Taiwan
[4] Department of Materials and Optoelectronic Science, National Sun Yat-sen University, Kaohsiung 804, Taiwan
[5] Cavendish Laboratory, University of Cambridge, J J Thomson Avenue, Cambridge CB3 0HE, United Kingdom

E-mail: ctliang@phys.ntu.edu.tw and ghkim@skku.edu

Received 4 May 2017, revised 11 June 2017
Accepted for publication 19 June 2017
Published 24 July 2017

Abstract

Temperature-driven flow lines are studied in the conductivity plane in a GaAs-based two-dimensional electron system containing self-assembled InAs dots when Landau level filling factor $\nu = 2$-4. In the insulator-quantum Hall (I-QH) transition resulting from the floating-up of the extended states, the flow diagram shows the critical behavior and we observed the expected semicircle in the strongest disorder case. By decreasing the effective disorder, we find that such flow lines can leave the I-QH regime and correspond to the plateau–plateau transition between $\nu = 4$ and 2. The evolution of the conductivity curve at low magnetic fields demonstrates the importance of Landau-level mixing to the semicircle when the extended states float up.

Keywords: insulating state, floating-up, semicircle

(Some figures may appear in colour only in the online journal)

1. Introduction

Quantum interference and Landau quantization can modulate the transport properties of a two-dimensional electron system (2DES) not only in the quantum Hall (QH) regime, but also in the Shubnikov-de Hass (SdH) transport regime [1, 2]. To understand the evolution of extended states to localized states in vanishing magnetic field B in a non-interacting, low-mobility system, Khmel'nitzkii [3] and Laughlin [4] proposed a picture of how extended states shift in energy. They argued that as B is decreased the extended states float up in energy and eventually rise above the Fermi energy. When there are no extended states below the Fermi energy, a 2DES is in the insulating state. The global phase diagram (GPD), which depends on disorder strength and B, is thus proposed according to the floating-up picture [5]. GPD describes a class of possible quantum phase transitions, namely the plateau–plateau (P–P) and insulator-quantum Hall (I-QH) transitions in the QH systems. It is worth pointing out that high-mobility devices near $B = 0$ can be irrelevant to GPD because of the finite sizes and/or temperatures [6, 7]. In high-mobility devices in which strong interactions can be present, near $B = 0$, metallic instead of insulating behavior can be observed [8].

[6] Authors to whom any correspondence should be addressed.

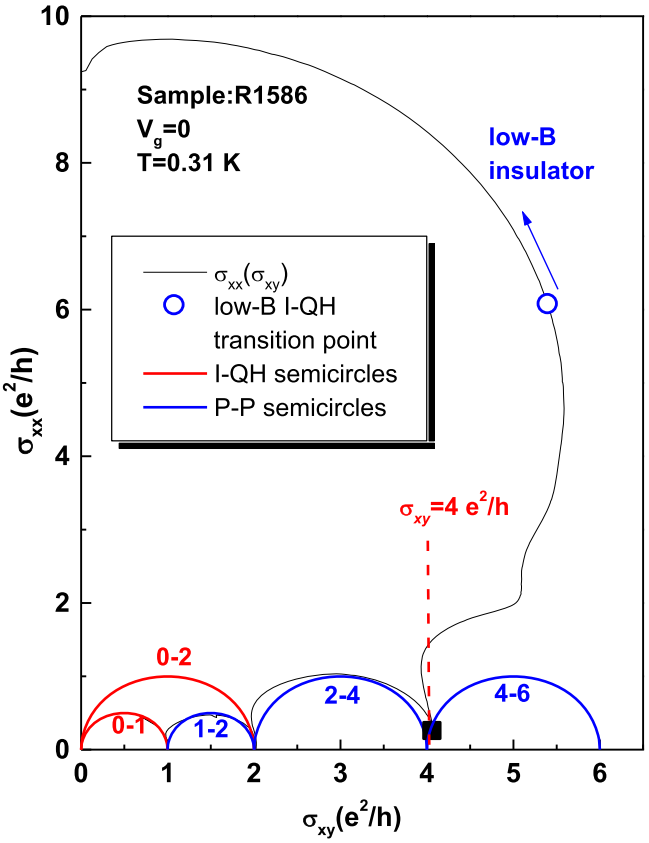

Figure 1. $\sigma_{xx}(\sigma_{xy})$ taken on a typical modulation-doped heterostructure showing the low-field insulator-quantum Hall transition. Theoretically predicted semicircles are indicated.

According to the finite size scaling theory, the critical behavior in such transitions reflects scaling $(\nu - \nu_c)/T^{\kappa}$ for both longitudinal and Hall conductivities σ_{xx} and σ_{xy} [9–12], where ν is the filling factor, κ is the critical exponent, ν_c is the filling factor at the critical point, σ_{xx} is longitudinal resistivity and σ_{xy} is Hall conductivity, respectively. On the other hand, by changing the temperature so as to vary the phase coherence length, which serves as an effective system size for scaling, the renormalization group or the T-driven flow diagram can be constructed [9, 13]. The T-driven flow diagram based on the semicircle law in the $(\sigma_{xy}, \sigma_{xx})$ plane is thus widely used to study the quantum phase transitions [9, 13–19]. For a spin-degenerate 2DES, it has been experimentally established that the flow lines in the conductivity plane follow $(\sigma_{xx})^2 + [\sigma_{xy} - (2n + 1)(e^2/h)]^2 = (e^2/h)^2$, where $n = 0, 1, 2\ldots$ is the Landau level index. In such a diagram, the unstable point at $(\sigma_{xy}, \sigma_{xx}) = ((2n + 1)e^2/h, e^2/h)$ represents a critical boundary, and the flow lines on its two sides flow in the opposite directions toward the stable points $(\sigma_{xy} = (2n)e^2/h, \sigma_{xx} = 0)$ corresponding to QH phases.

A pioneering numerical study showed that Landau-level mixing effects can strongly modify the scaling functions and distort the corresponding semicircles in weak magnetic fields [20]. However, the scaling relation may be destroyed when using such numerical methods. Besides, numerically it is difficult to understand the floating-up extended states. Therefore it is desirable to study the Landau-level mixing effects on the scaling and semicircle law from the experimental measurements. To this end, we study the T-driven flow lines in the $(\sigma_{xy}, \sigma_{xx})$ plane in a low-mobility GaAs-based 2DES with self-assembled InAs dots when Landau level filling factor $\nu = 2$–4. In the I-QH transition resulting from the floating-up extended states, we observed the critical behavior following the expected semicircle by constructing the flow diagram. By decreasing the effective disorder, we found that such flow lines can leave the I-QH regime and correspond to the P–P transition between $\nu = 4$ and 2. The evolution of the curve $\sigma_{xx}(\sigma_{xy})$ at low B demonstrated the importance of Landau-level mixing to the semicircle in the observed I-QH transition. In addition, our study showed the survived scaling features when the universal scaling is invalid.

2. Experimental details

The samples used in this study are GaAs/AlGaAs 2DESs containing self-assembled InAs quantum dots grown by molecular beam epitaxy which have been reported before [21–24]. The layer sequence was grown on a GaAs (100) substrate as follows: 50 nm AlGaAs, 20 nm GaAs where 2.15 monolayers of InAs capped by a 5 nm GaAs layer, 40 nm undoped AlGaAs, 40 nm Si doped AlGaAs, and a 17 nm GaAs cap layer. The self-assembled InAs quantum dots in our system introduce short-range disorder [25–27] and provide necessary scattering for observing the I-QH transition [26–29]. Hall bar configuration was made by standard lithography and etching process and Au/Ni/Cr was deposited as the front-gate. By applying the front-gate voltage V_g, one can vary the two-dimensional carrier density n. As n increases, the electron gas becomes progressively able to screen the disorder potential, and therefore the effective disorder of the sample can be controlled by changing V_g [30, 31]. We estimate that the InAs dot density is about 18 μm^{-2}. The length and width of the Hall bar device are 640 μm and 80 μm, respectively. Four-terminal longitudinal (ρ_{xx}) and Hall (ρ_{xy}) resistivity measurements were performed using standard phase-sensitive lock-in techniques and a driving current of 10 nA was applied to the sample. Conductivities σ_{xx} and σ_{xy} can be obtained by inverting the resistivity tensor $\sigma_{xx(xy)} = \rho_{xx(xy)}/(\rho_{xx}^2 + \rho_{xy}^2)$. Experiments were performed in a top-loading He^3/He^4 dilution refrigerator (Device 1) and a top-loading He^3 cryostat (Device 2). We use the high-temperature Hall effect and resistivity data to characterize the sample parameters so that the highly insulating behavior due to strong localization can be the less pronounced. For Device 1, at $V_g = -0.274$ V, the carrier density is estimated to be $6.5 \times 10^{10}\,cm^{-2}$ and mobility is $2000\,cm^2\,V^{-1}\,s^{-1}$. For Device 2, at $V_g = -0.02$ V, -0.06 V, -0.09 V and -0.1035 V, the carrier density (mobility) is $1.18 \times 10^{11}\,cm^{-2}$, $9.08 \times 10^{10}\,cm^{-2}$, $6.69 \times 10^{10}\,cm^{-2}$ and $5.98 \times 10^{10}\,cm^{-2}$ ($18600\,cm^2\,V^{-1}\,s^{-1}$, $11900\,cm^2\,V^{-1}\,s^{-1}$, $6260\,cm^2\,V^{-1}\,s^{-1}$, and $3060\,cm^2\,V^{-1}\,s^{-1}$), respectively.

3. Results and discussions

Before describing our main experimental data, we present data taken on a typical modulation-doped GaAs/AlGaAs heterostructure. The carrier density is $2.0 \times 10^{11}\,\mathrm{cm}^{-2}$ and the mobility is $7600\,\mathrm{cm}^2\,\mathrm{V}^{-1}\,\mathrm{s}^{-1}$. The sample structure can be found in [18]. Figure 1 shows $\sigma_{xx}(\sigma_{xy})$ at the lowest measurement temperature $T = 0.31$ K. The blue open point close to $(5.5e^2/h,\ 6e^2/h)$ indicates the low-field I-QH transition, which separates the QH regime from the low-B insulator near zero magnetic field, and the arrow indicates the direction with decreasing B. The curve $\sigma_{xx}(\sigma_{xy})$ corresponds to the low-B insulator when $\sigma_{xx} > 6e^2/h$, under which there is no magneto-oscillation. For $\sigma_{xx} < 6e^2/h$, the sample enters the QH regime. In the high-B regime where $\sigma_{xy} \leqq 2e^2/h$, we can see a spin-split 2-1 transition well approximated by the semicircle. For even higher B, we can observe a portion of the $\nu = 1$-insulator semicircle. The deviation from the semicircle law is small in the 4-2 transition, and the solid square corresponding to the minimum value of σ_{xx} near $\nu = 4$ close to the expected point $(4e^2/h,\ 0)$ in the conductivity plane. The deviation from the semicircle for the filling factor range $\nu = 4$–6, however, becomes significant and we can see from figure 1 that $\sigma_{xy}(\sigma_{xx})$ is distorted to the red dashed line $\sigma_{xy} = 4e^2/h$ just as such a curve leaves the solid square with decreasing B. We note that the cyclotron gap, which separates adjacent Landau bands, is reduced with decreasing B and thus Landau-level mixing is expected. The distortion in $\nu = 4$–6, in fact, supports Ando's prediction [20] on the decrease of the Hall conductivity under such mixing.

Although the semicircle law is valid in the QH regime in figure 1, the value of σ_{xx} at low magnetic field is much higher than e^2/h and the low-B insulator is irrelevant to GPD [32]. Therefore, the curve $\sigma_{xx}(\sigma_{xy})$ near the low-B I-QH transition deviates very much from the 0-1 or 0-2 semicircle expected for the I-QH transition following GPD. On the other hand, device 1 is suitable for probing the insulating phase in GPD at low B when the extended states float up [22]. Figure 2(a) shows the magneto-transport data of longitudinal resistivity ρ_{xx} for gate voltage $V_g = -0.276$ V at various temperatures (Device 1). Magneto-oscillations are present in the low-B insulator. Device 1 shows the insulator to $\nu = 2$ QH transition (figure 2(b)). The expected semicircle and the features of scaling in the floating-up extended states were observed from the T-driven flow diagram, as shown in figure 2(c). However, the curve deviates from the semicircle at low magnetic fields, which can be ascribed to SdH-like magneto-oscillations [22], which do not appear in the low-B insulator in figure 1. The SdH-like magneto-oscillations suggest the existence of the semiclassical Landau quantization at low B, where different Landau levels may mix because of the small level separation [32], under the floating-up extended states in Device 1.

In order to further study the Landau-level mixing effect, we perform a systematic study on another device with an identical sample layer sequence (Device 2). Figures 3(a)–(c) show the T-driven flow lines in the conductivity plane for $V_g = -0.06$ V, -0.09 V and -0.1035 V, respectively. In the following we denote the spin-degenerate P–P and I-QH

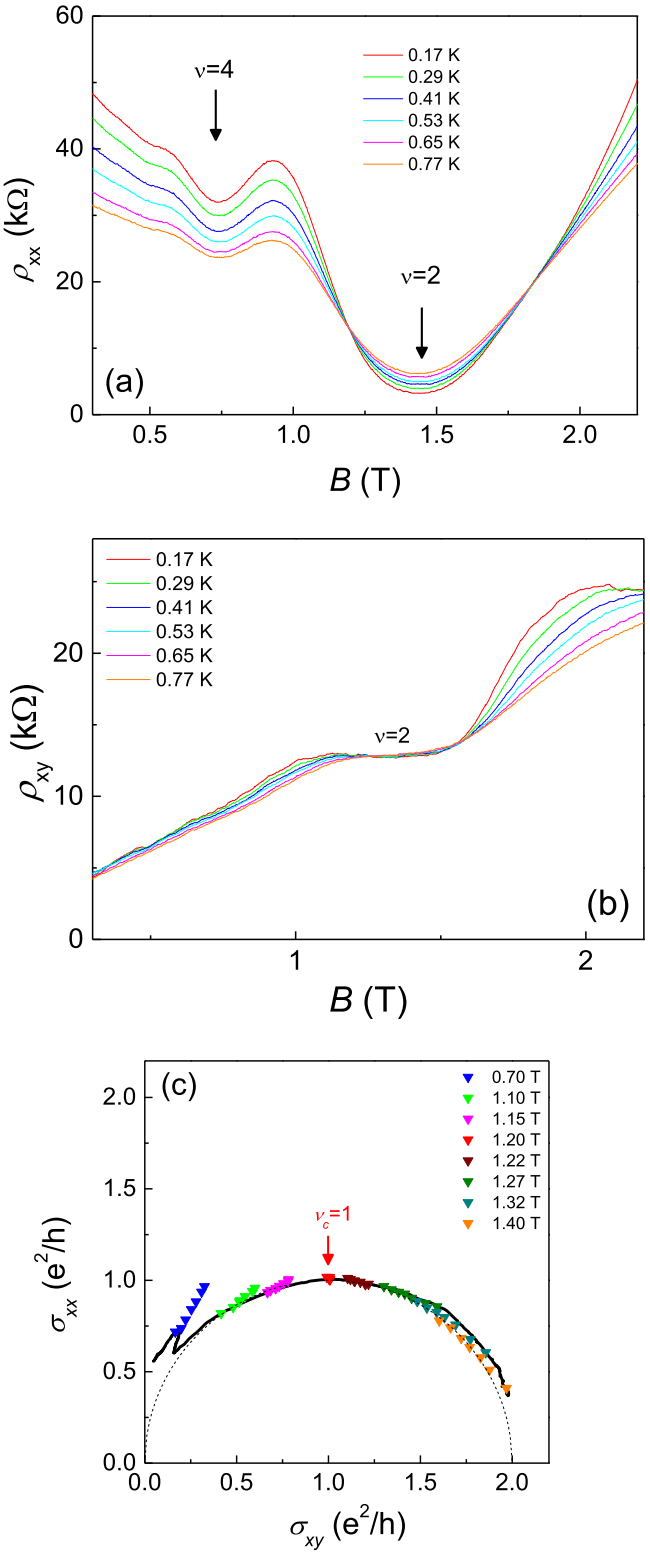

Figure 2. (a) Longitudinal resistivity for gate voltage $V_g = -0.276$ V at various temperatures. SdH-like oscillations are present in the low field region. (b) Hall resistivity as a function of B. (c) The T-driven flow lines. The black curve $\sigma_{xx}(\sigma_{xy})$ is taken at $T = 0.17$ K. (Device 1).

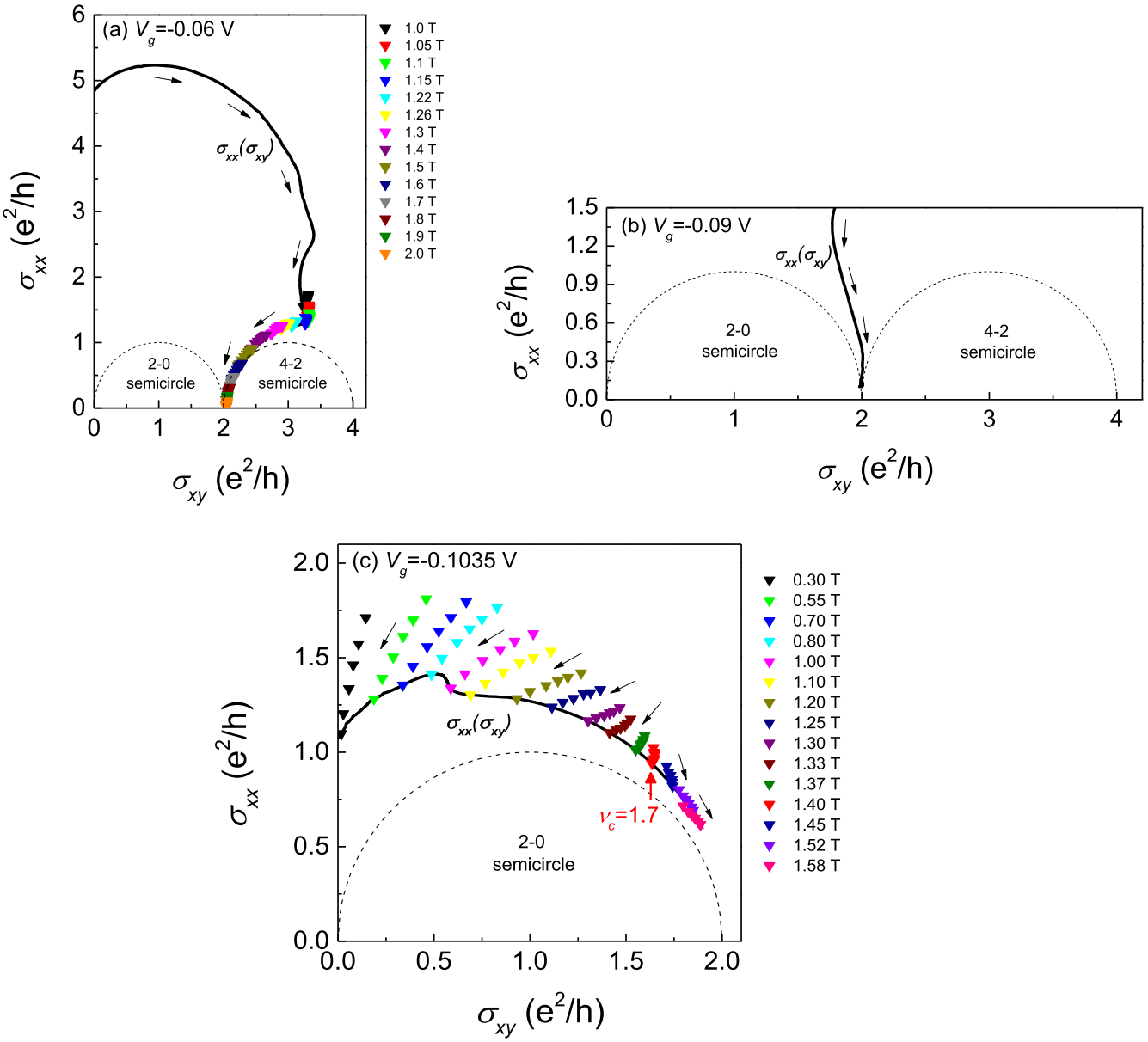

Figure 3. The T-driven flow lines at (a) $V_g = -0.06$ V; measurement temperatures: $T = 1.37$, 1.08, 0.93, 0.78, 0.61, 0.47, 0.32 and 0.25 K. The solid curve corresponds to $\sigma_{xx}(\sigma_{xy})$ at the lowest temperature ($T \sim 0.25$ K). (b) $V_g = -0.09$ V ($T = 0.25$ K); (c) $V_g = -0.1035$ V; measurement temperatures: $T = 1.51$, 1.03, 0.89, 0.68, 0.50 and 0.32 K. The solid curve corresponds to $\sigma_{xx}(\sigma_{xy})$ at the lowest temperature ($T \sim 0.32$ K). (Device 2).

transitions as the 4-2 and 2-0 transitions, where the number 4, 2, and 0 represent the QH states of $\nu = 4$ and 2 and the insulating states, respectively. The triangles labeled by the same color correspond to the data at a fixed magnetic field. The arrows indicate the flow direction with decreasing temperature at fixed B and the solid line is the curve $\sigma_{xx}(\sigma_{xy})$ at the lowest temperature ($T \sim 0.25$ K). The dotted curves are the theoretical prediction of semicircles for 4-2 and 2-0 transition. At $V_g = -0.06$ V, as seen in figure 3(a), the sample shows a crossover from semiclassical to QH transport [33], and the value of σ_{xx} at low B is much higher than e^2/h just as that in figure 1. With increasing magnetic fields, the system enters the QH regime ($\nu = 4$-2) and we observed that the curve $\sigma_{xx}(\sigma_{xy})$ becomes closer to the expected 4-2 semicircle as the flow lines approach the QH state at $(2e^2/h, 0)$. As V_g decreases, as shown in figure 3(b), the curve $\sigma_{xx}(\sigma_{xy})$ leaves the 4-2 semicircle and follows along a vertical line ($\sigma_{xy} = 2e^2/h$) because of the decrease of the Hall conductivity σ_{xy}, which is similar to the distortion near the solid square in figure 1 as $\nu = 4$-6 just as what is mentioned above, the decrease of the Hall conductivity supports Ando's prediction [20] about the Landau-level mixing. When V_g is further reduced to -0.1035 V, the data which has been presented by previous study [23] is shown to have a 2-0 transition as $\nu = 4$-2, where σ_{xy} decreases more and indicates stronger level mixing. As seen in figure 3(c), the vertical flow denoted by red triangles shows the crossing magnetic field and the curves on its two sides move in opposite directions toward

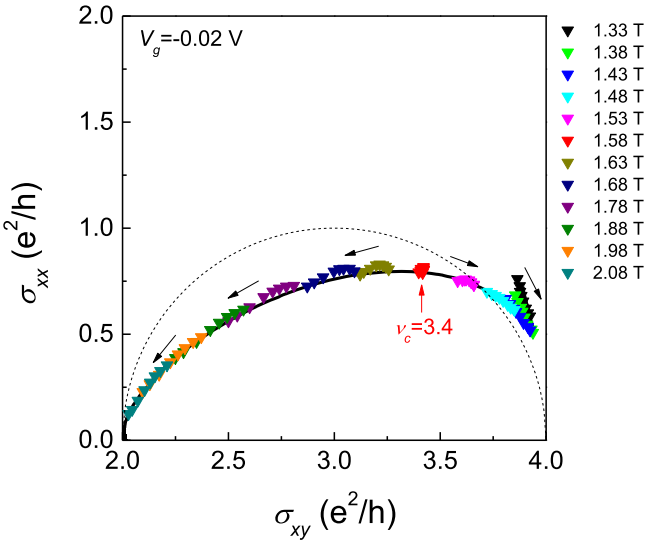

Figure 4. The T-driven flow diagram with a crossing point denoted by red triangles at $\nu_c = 3.4$ for $V_g = -0.02$ V. Measurement temperatures: $T = 1.6$, 1.3, 1.07, 0.90, 0.71, 0.52, 0.36 and 0.25 K. $\sigma_{xx}(\sigma_{xy})$ at $T = 0.25$ K is shown in the solid curve. (Device 2).

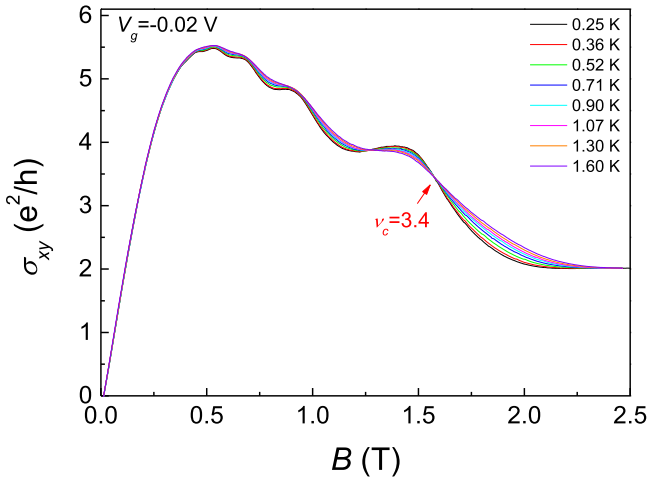

Figure 5. σ_{xy} as a function of B at various temperatures with a crossing point at $\nu_c = 3.4$ for $V_g = -0.02$ V. (Device 2).

$(2e^2/h, 0)$ and $(0, 0)$, respectively. The observed 2-0 transition is consistent with a GPD in the context of the floating-up of the lowest energy level for a spin-degenerate 2DES. For the most disordered case ($V_g = -0.1035$ V), the semicircle in the observed 2-0 transition is in fact originated from the distortion on the plateau-transition curve due to Landau-level mixings.

In addition to the T-driven flow diagram governed by the semicircle law, universal scaling function as well as universal exponent are fundamental for an understanding of quantum phase transitions [9, 10, 34–38]. It has been shown that σ_{xy} is the more important quantity [36] in the study of the scaling theory since the critical point in σ_{xy} is more robust than that in σ_{xx} with respect to T [15, 34]. The scaling behaviors can be examined near each transition point by $\sigma_{xy} = f((\nu - \nu_c)/T^{\kappa})$ and $|\mathrm{d}\sigma_{xy}/\mathrm{d}B| \propto T^{-\kappa}$, where f is the scaling function, ν is the filling factor, κ is the critical exponent, and ν_c is the filling factor at the critical point [22, 37, 39]. For further examination, we present the data at $V_g = -0.02$ V. The T-driven flow diagram shows scaling behavior in the sense that the flow is on top of those taken at the lowest measurement temperature as well as the unstable point, as shown in figure 4. Such a crossing point defined by the T-independent point in the plot of $\sigma_{xy}(B)$ is also observed at $\nu_c = 3.4$ as shown in figure 5. It is common to examine the universality of κ for studying the quantum phase transitions [9, 10, 39, 40]. By plotting $\ln|\mathrm{d}\sigma_{xy}/\mathrm{d}B|$ versus $\ln T$ near the critical points $\nu_c = 3.4$, and $\nu_c = 1.7$ as shown in figures 6(a) and (b), $\kappa = 0.26$ and $\kappa = 0.27$ can be obtained from the slope of the linear fits for $V_g = -0.02$ V and $V_g = -0.1035$ V, respectively. In a spin-degenerate system, κ is expected to be 0.21 [9, 10, 39]. The value of κ from our result deviates from the expected universal value. The discussion on the deviation in κ from the universal value has been reported [40], and is beyond the scope of this paper. Here, we focus on the correspondence between the scaling behavior in the flow diagram and the

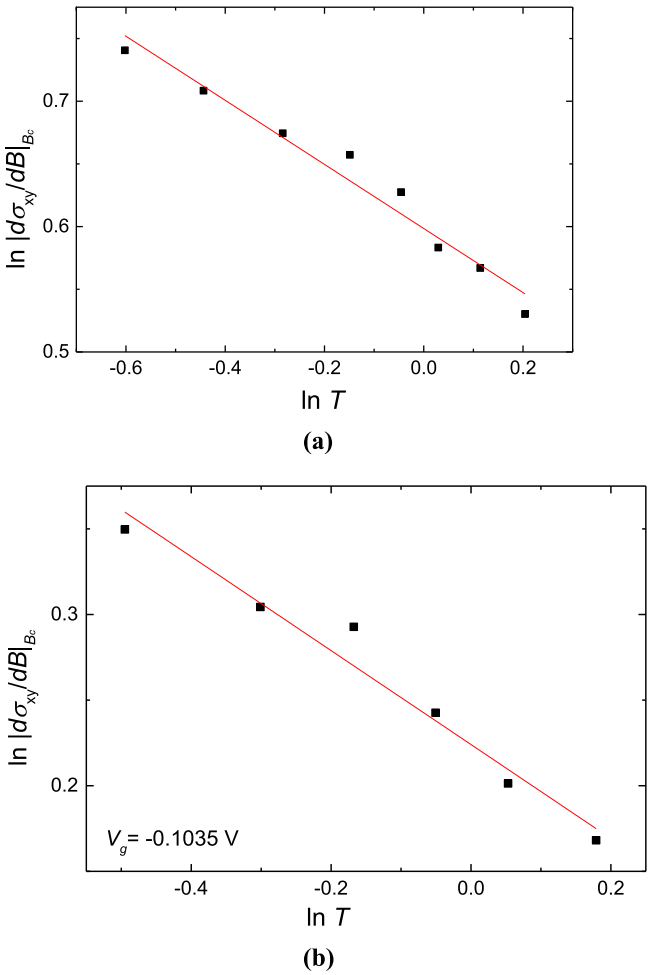

Figure 6. (a) $\ln(\mathrm{d}\sigma_{xy}/\mathrm{d}B)$ versus $\ln T$ for $V_g = -0.02$ V, where $\kappa = 0.26$ is obtained from the slope of the linear fit. (b) $\ln(\mathrm{d}\sigma_{xy}/\mathrm{d}B)$ versus $\ln T$ for $V_g = -0.1035$ V, where $\kappa = 0.27$ is obtained from the slope of the linear fit. (Device 2).

universal scaling function. The deviation in κ reveals that the universal scaling is not found in our sample even though the T-driven flow diagram shows the scaling behavior and the semicircle relation. In our experimental study, therefore, we found that survived scaling features can still be observed under the invalidity of the expected universal scaling.

There are reports on the Landau-level mixing at high magnetic fields in Si/SiGe two-dimensional hole systems, where transitions forbidden in the GPD can be observed [41, 42]. On the other hand, the mixing effects in Devices 1 and 2 in our study are observed in the 0-2 I-QH transitions following the GPD as the extended states float up at low B. While the semicircle law is valid in the low-B I-QH transitions in these two devices, we note from figure 1 that the curve $\sigma_{xx}(\sigma_{xy})$ at low B may deviate greatly from the semicircles in the transition irrelevant to the GPD.

4. Conclusions

We have studied the T-driven flow lines corresponding to Landau level filling factor $\nu = 2$–4 in the σ_{xx}–σ_{xy} plane in a GaAs-based 2DES with self-assembled InAs dots. The flow diagram can follow the 0-2 semicircle when the extended states float up and induce the low-B I-QH transition in the GPD, and our study shows the importance of Landau-level mixing to the semicircle law under the floating-up extended states. While the flow lines show the scaling behavior, the universality in κ is not found, showing that surviving scaling features can still be observed when the universal scaling is invalid. We plan to extend this concept to the fractional QH regime [43] and other disordered systems [44–48].

Acknowledgments

We would like to thank T-M Chen, Y-H Chiu, C P Huang, T-Y Huang, J R Juang, Hao Hsiung Lin, M-G Lin, J T Nicholls and H-S Wang for their experimental help at an early stage of this work. This research was supported by the Basic Science Research Program through the National Research Foundation of Korea (NRF) funded by the Ministry of Education, Science and Technology (2016R1A2A2A05921925). C-TL acknowledges the support from the Ministry of Science and Technology (MOST), Taiwan (Grant number: MOST 105-2119-M-002-048-MY3).

References

[1] Abrahams E, Anderson P W, Licciardello D C and Ramakrishnan T V 1979 *Phys. Rev. Lett.* **42** 673
[2] von Klitzing K, Dorda G and Pepper M 1980 *Phys. Rev. Lett.* **45** 494
[3] Khmelnitskii D 1984 *Phys. Lett.* A **106** 182
[4] Laughlin R B 1984 *Phys. Rev. Lett.* **52** 2304
[5] Kivelson S, Lee D-H and Zhang S C 1992 *Phys. Rev.* B **46** 2223
[6] Huckestein B 2000 *Phys. Rev. Lett.* **84** 3141
[7] Hang D R, Huang C F, Zhang Y W, Yeh H D, Hsiao J C and Pang H L 2007 *Solid State Commun.* **141** 17
[8] Spivak B, Kravchenko S V, Kivelson S A and Gao X P A 2010 *Rev. Mod. Phys.* **82** 1743
[9] Pruisken A M M 1988 *Phys. Rev. Lett.* **61** 1297
[10] Wei H P, Tsui D C, Paalanen M A and Pruisken A M M 1988 *Phys. Rev. Lett.* **61** 1294
[11] Huckestein B 1995 *Rev. Mod. Phys.* **67** 357
[12] Sondhi S L, Girvin S M, Carini J P and Shahar D 1997 *Rev. Mod. Phys.* **69** 315
[13] Wei H P, Tsui D C and Pruisken A M M 1986 *Phys. Rev.* B **33** 1488
[14] Burgess C P, Dib R and Dolan B P 2000 *Phys. Rev.* B **62** 15359
[15] Dolan B P 2000 *Phys. Rev.* B **62** 10278
[16] Lütken C A and Ross G G 1993 *Phys. Rev.* B **48** 2500
[17] Murzin S S, Weiss M, Jansen A G M and Eberl K 2002 *Phys. Rev.* B **66** 233314
[18] Huang C F, Chang Y H, Cheng H H, Yang Z P, Yeh H D, Hsu C H, Liang C-T, Hang D R and Lin H H 2007 *J. Phys.: Condens. Matter* **19** 026205
[19] Wang Y-T *et al* 2012 *J. Phys.: Condens. Matter* **24** 405801
[20] Ando T 1986 *J. Phys. Soc. Japan* **55** 3199
[21] Kim G H, Nicholls J T, Khondaker S I, Farrer I and Ritchie D A 2000 *Phys. Rev.* B **61** 10910
[22] Kim G H, Liang C-T, Huang C F, Nicholls J T, Ritchie D A, Kim P S, Oh C H, Juang J R and Chang Y H 2004 *Phys. Rev.* B **69** 073311
[23] Huang T-Y, Huang C F, Kim G H, Huang C-P, Liang C-T and Ritchie D A 2009 *Chin. J. Phys.* **47** 401
[24] Huang T-Y, Liang C-T, Kim G H, Huang C F, Huang C-P and Ritchie D A 2010 *Physica* E **42** 1142
[25] Sales D L, Sanchez A M, Beanland R, Henini M and Molina S I 2007 *Semicond. Sci. Technol.* **22** 168
[26] Li W, Vicente C L, Xia J S, Pan W, Tsui D C, Pfeiffer L N and West K W 2003 *Appl. Phys. Lett.* **83** 2832
[27] Li W, Vicente C L, Xia J S, Pan W, Tsui D C, Pfeiffer L N and West K W 2003 *Phys. Rev. Lett.* **102** 216801
[28] Song S-H, Shahar D, Tsui D C, Xie Y H and Monroe D 1997 *Phys. Rev. Lett.* **78** 2200
[29] Jiang H W, Johnson C E, Wang K L and Hannahs S T 1993 *Phys. Rev. Lett.* **71** 1439
[30] Das Sarma S, Lilly M P, Hwang E H, Pfeiffer L N, West K W and Reno J L 2005 *Phys. Rev. Lett.* **94** 136401
[31] Shahar D, Tsui D C and Cunningham J E 1995 *Phys. Rev.* B **52** 14372
Walter Schirmacher W, Fuchs B, Höfling F and Franosch T 2015 *Phys. Rev. Lett.* **115** 240602
[32] Isihara A and Smrcka L 1986 *J. Phys. C: Solid State Phys.* **19** 6777
[33] Pruisken A M M 2010 *Int. J. Mod. Phys.* B **24** 1895
[34] Huo Y, Hetzel R E and Bhatt R N 1993 *Phys. Rev. Lett.* **70** 481
[35] Shahar D, Tsui D C, Shayegan M, Shimshoni E and Sondhi S L 1997 *Phys. Rev. Lett.* **79** 479
[36] Pallecchi E, Ridene M, Kazazis D, Lafont F, Schopfer F, Poirier W, Goerbig M O, Mailly D and Ouerghi A 2013 *Sci. Rep.* **3** 1791
Huang L-I, Yang Y, Elmquist R E, Lo S-T, Liu F-H and Liang C-T 2016 *RSC Adv.* **6** 71977
[37] Huang C F, Chang Y H, Lee C H, Chou H T, Yeh H D, Liang C-T, Chen Y F, Lin H H, Cheng H H and Hwang G J 2002 *Phys. Rev.* B **65** 045303
[38] Hughes R J F, Nicholls J T, Frost J E F, Linfield E H, Pepper M, Ford C J B, Ritchie D A, Jones G A C, Kogan E and Kaveh M 1994 *J. Phys.: Condens. Matter* **6** 4763
[39] Wang T, Clark K P, Spencer G F, Mack A M and Kirk W P 1994 *Phys. Rev. Lett.* **72** 709

[40] Koch R, Haug R J, von Klitzing K and Ploog K 1991 *Phys. Rev.* B **43** 6828
[41] Sakr M R, Rahimi M, Kravchenko S V, Coleridge P T, Williams R L and Lapointe J 2001 *Phys. Rev.* B **64** 161308(R)
[42] Liang C-T, Huang C F, Cheng Y-M, Huang T-Y, Chang Y H and Chen Y F 2001 *Chin. J. Phys.* **39** L305
[43] Diankov G *et al* 2016 *Nat. Commun.* **7** 13908
[44] Lu Y-F *et al* 2013 *ACS Nano* **7** 6522
[45] Yang W Y *et al* 2016 *Semicond. Sci. Technol.* **31** 115001
[46] Liu C-I *et al* 2016 *Semicond. Sci. Technol.* **31** 105008
[47] Hang D R *et al* 2001 *Appl. Phys. Lett.* **79** 66
[48] Wang Y-T *et al* 2016 *J. Korean Phys. Soc.* **65** 1503